WPMAT-PR(17) 18640

F Granberg et al.

Effect of Obstacle Nanostructure on the Movement of Edge Dislocations in BCC FE

Preprint of Paper to be submitted for publication in
Journal of Nuclear Materials

This work has been carried out within the framework of the EUROfusion Consortium and has received funding from the Euratom research and training programme 2014-2018 under grant agreement No 633053. The views and opinions expressed herein do not necessarily reflect those of the European Commission.

Available online at www.sciencedirect.com

ScienceDirect

Journal of Nuclear Materials 00 (2017) 1–5

EFFECT OF OBSTACLE NANOSTRUCTURE ON THE MOVEMENT OF EDGE DISLOCATIONS IN BCC FE

F. Granberg[a,*], K. Nordlund[a]

[a]*Department of Physics, P.O. Box 43, FIN-00014 University of Helsinki, Finland*

Abstract

In this study we investigate how different obstacle nanostructures affect the edge dislocation movement in an iron matrix by molecular dynamics simulations. We investigate the effect of temperature, nanostructure, size of the obstacle and composition of the obstacle on the unpinning stress. We investigated three different obstacles of three different sizes at five different temperatures, and compared them with four previously studied obstacles. All simulations were performed in the same system setup, with the same parameters, to ensure comparable results. At the two smaller sizes 1 nm and 2 nm, the differences between different kinds of obstacles was not so large, but some variations could be seen. For the 4 nm obstacles we clearly see four different groupings of unpinning stresses. This suggested that they did have different unpinning mechanisms, which was also confirmed by visual analysis. The same mechanisms were also seen for most the smaller obstacles within the same kind, even though the unpinning stresses did not differ too much. The effect of multiple interactions is also investigated, where the same dislocation was passing through the same obstacles. Other general trends observed, were that a larger obstacle will require a higher stress for the edge dislocation to unpin, and that an increase in temperature will lower the needed unpinning stress.

Keywords:
dislocation, molecular dynamics, precipitate

1. Introduction

In demanding environments, like nuclear power plants, the mechanical properties of the structural materials is crucial to know. These demanding environments can be due to the constant radiation present or the loading and unloading of the structural materials. Most structural parts are made from some variety of steel, which has a complex nanostructure of precipitates, grains, inclusions and alloying elements. The complex nanostructure is the key to the good mechanical and other properties of steels, and therefore further improvements by informed choices can probably be made. The mechanical properties of metals are determined by the movement of dislocations and the interaction of the dislocations with the different features. Therefore it is important to know how the dislocations are interacting with the different features, to be able to predict the properties of the material.

The dislocations are usually pinned by the obstacles and there is a certain stress at which the dislocation can unpin from the obstacle. The unpinning stress is one of the parameters important to know to enable larger-scale dislocation modelling. Another important parameter to know is the mechanism that is present when the dislocation is unpinning from the obstacle. The unpinning stress will determine the immediate strength of the obstacle. Different mechanisms will, on the other hand, determine the evolution of both the dislocation and the obstacle. Some interaction mechanisms will destroy the obstacle and therefore make the material softer and some mechanisms will make the material stronger, but also more brittle. Both of these can have detrimental consequences, if the phenomenon is not known or expected. These two parameters, which are related to each other, are a result of the interaction of dislocations with obstacles on an atomic scale, which is why molecular dynamics simulations are well suited to study both of these. These results can be used as parameters in higher scale models, such as dislocation dynamics. The unpinning stress can be used to adjust the strength of obstacles [1] and the obstacle can be adjusted so that the right mechanism is present. The different mechanism and setups to achieve these in dislocation dynamics have been studied previously [2, 3, 4].

In this Article, we focus on the unpinning stress needed for the edge dislocation to unpin from different kinds of obstacles and how different factors, like size and temperature, will change the pinning strength. The unpinning mechanism will also be de-

*Corresponding author.
Email address: fredric.granberg@helsinki.fi (F. Granberg)

termined to get a better understanding of how these two parameters relate to each other. We have investigated and compared seven different obstacles in pure iron, to determine the unpinning stress for edge dislocations, by means of classical molecular dynamics (MD) simulations. The effect of obstacle size and temperature on the unpinning stress is also investigated. All simulations are conducted in the same system setup and the same input parameters are used to ensure comparability between the results of the different obstacles.

2. Methods

The simulations were performed with the classical MD code PARCAS [5, 6], with an interatomic potential, describing Fe, Cr and C interactions, by Henriksson *et al.* [7]. The simulation setup was according to the setup described in Ref. 8, by Osetsky and Bacon. The *x*-, *y*- and *z*-axis were oriented along the [111], $[\bar{1}\bar{1}2]$ and $[1\bar{1}0]$-directions, respectively, in the BCC structured simulation cell. An edge dislocation with the Burgers's vector $\mathbf{b} = 1/2[111]$ was generated in the $x-y$ slip plane. The dislocation was generated by placing N layers in the top half and $N-1$ layers in the bottom half, and then compressing and extending the halves by the Burger's vector divided by two to match the two halves. This will introduce a perfect edge dislocation in the middle of the cell. A few layers of atoms were fixed in the top and the bottom-part of the *z*-direction, and a Berendsen type thermostat [9] was applied on a few layers of atoms above the fixed atoms at the bottom.

The fixed layers at the top were moved by a constant strain rate of 5×10^7 s^{-1} in the *x*-direction, to induce a glide force on the edge dislocation. A schematic illustration of the system setup can be seen in Fig. 1, where the gray boxes are the fixed regions and the gray plane the slip plane where the dislocation is moving in. The pristine box with the pre-existing edge dislocation contained 542,700 atoms, which was the starting point for the generation of the simulation cells with the different obstacles. The box was 101×3, 30×6 and 30×2 atomic planes in *x*-, *y*- and *z*-directions, respectively. This resulted in a box size of $25 \times 21 \times 12$ nm^3. Periodic boundary conditions were applied in the *x*- and *y*-directions. Due to the periodic boundary conditions, the distance between the obstacles was 21 nm $- d_p$, where d_p is the diameter of the obstacle. The same box size and strain rate have been used in previous studies, and some of the results are taken from them, Refs. 10 and 11.

In the investigation of the size effect we used three different obstacle sizes, 1 nm, 2 nm and 4 nm, and the temperatures studied were 300 K, 450 K, 600 K, 750 K and 900 K. The used potential and strain rate showed a temperature dependent stress for steady-state glide of the dislocation. This value has been subtracted from the numerical results, to get the contribution of only the obstacles. The stress for steady-state glide was 90 MPa, 85 MPa, 80 MPa, 75 MPa and 70 MPa for the increasing temperature. To visualize the interaction of the dislocation with the obstacle the program OVITO [12], and the Adaptive Common Neighbor Analyzis implemented in the program, were used.

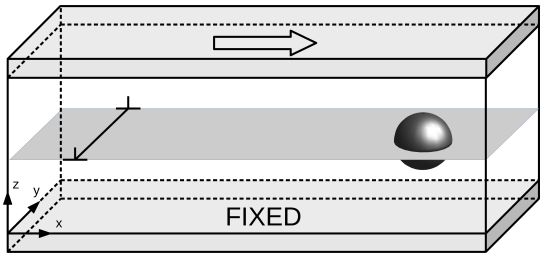

Figure 1. Schematic illustration of the system setup.

The investigated obstacles were: voids, coherent chromium precipitates, amorphous cementite precipitates (amorphous Fe_3C), which are compared to previously studied cementite (Fe_3C), $Fe_{23}C_6$, $Cr_{23}C_6$ precipitates and cementite rods [10, 11]. The results for the unpinning stresses for spherical cementite, $Fe_{23}C_6$- and $Cr_{23}C_6$-precipitates and the cementite rods are taken from Refs. 10 and 11. All obstacles except the cementite rods were spherical, and the rods were cylindrical with the axis perpendicular to the slip plane, and were almost as long as the height between the fixed layers [10]. In the simulation of the voids and coherent chromium precipitates the amount of atoms in the obstacles were 44, 349 and 2775 vacancy/chromium atoms for the 1 nm, 2 nm and 4 nm obstacles, respectively. All simulations were conducted with three different initial seeds, to investigate the stochastic part of the unpinning events. The exceptions was the amorphous cementite. For the amorphous cementite simulations, three different amorphous structures were investigated, in addition to three different initial seeds for one of the investigated structures. All the unpinning stresses given in the Results section are averages of three initial seeds/structures.

3. Results and Discussion

3.1. Unpinning stress and mechanism

The unpinning stresses for all obstacles can be seen in Figs. 2, 3 and 4, for the 1 nm, 2 nm and 4 nm obstacles, respectively. The first general trend that can be seen is that an increasing temperature has a lowering effect on the unpinning stress, which has been seen in previous studies [13, 14, 15, 16]. Another general trend observed before is that a larger obstacle will yield a higher unpinning stress [13, 14, 15, 16]. The only exception in the used potential is the coherent chromium precipitates, where these two conclusions are not evident. The difference between the different seeds for the same obstacles showed very small differences. Mainly the difference was seen for the small sizes and at low temperature, where the stochastic movement of atoms that triggers the unpinning event is not present as often as at higher temperatures [10].

In previous studies it was shown that three different carbides, cementite, $Fe_{23}C_6$ and $Cr_{23}C_6$, of sizes 2 nm and 4 nm showed similar unpinning stresses [10]. There were a larger difference between the 1 nm spherical $Fe_{23}C_6$ compared to the others, which will be discussed later. As seen in Ref. 10 the cementite rod did show a higher unpinning stress than all of the

other carbides, which showed the importance of surface curvature on the unpinning phenomenon. The absorption of vacancies did in the case of the spherical obstacle lead to a smaller effective size of the obstacle, which explains the lower unpinning stress for the spherical cementite compared to the cylindrical.

If the results for the amorphous cementite are compared with spherical carbides previously studied [10, 11], cementite, $Fe_{23}C_6$ and $Cr_{23}C_6$, we see that the amorphous cementite agrees very well with the previous results. For the 2 nm and 4 nm obstacles we see almost the same results, and all of them showed the Orowan mechanism when unpinning [17]. The cementite rod also showed the Orowan unpinning mechanism, but the rod required a higher unpinning stress compared to the spherical cementite precipitates, due to the lack of surface curvature [10]. For the 1 nm amorphous cementite obstacles, the unpinning stress is on average a little bit lower than the cementite and $Cr_{23}C_6$, but higher than the $Fe_{23}C_6$. At the two larger sizes the difference between different amorphous regions did not affect the unpinning stress any more than the difference in stress due to different seeds. For the 1 nm amorphous region, the different seeds did not affect the unpinning stress any more than for other obstacles, but the different amorphous regions did drastically affect the results. This shows that some of the small obstacles were more stable than others and this can explain the difference in unpinning stress between the amorphous cementite obstacles and the other carbides. We saw that some of the amorphous cementites showed the Orowan mechanism and some of them shearing. The results showed that those with the Orowan mechanism showed a much higher unpinning stress compared to those that showed shear. Those with the Orowan mechanism showed the same unpinning stress as the crystalline cementite.

For the 1 nm $Fe_{23}C_6$ we saw shearing in all of the cases, which explains why the unpinning stress is lower than for the cementite. The unpinning stress for the 1 nm $Fe_{23}C_6$ is comparable with that of amorphous cementite with the shearing mechanism. Also the 1 nm $Cr_{23}C_6$ were sheared, but still showed a higher unpinning stress. This can probably be explained by the weaker bonding between Fe-C than Cr-C and the larger distortion created between the Cr atoms in the Fe matrix compared to Fe atoms in a Fe matrix.

The results show that the void has about the same pinning strength as the carbides for the 1 nm and 2 nm voids. For the size of 4 nm, however, we see a significantly lower unpinning stress for the voids compared to the 4 nm carbides, about 100 MPa to 200 MPa. All the voids had an attractive force on the dislocation, which absorbed the dislocation. This can be explained by the minimization of the length of the dislocation. This absorption then acted as an obstacle, because a new segment of the dislocation must be created before it can unpin from the void. This means that the larger voids had a larger attraction, but also resulted in a larger segment being created, hence the larger voids acted as stronger obstacles than the smaller voids.

All the coherent chromium precipitates show similar unpinning stresses independent of size, in some cases we even see that the smallest precipitates are stronger than the largest precipitates, at low temperature, see Fig. 5. The almost inverse size dependence of the chromium precipitates are in contradiction to other studies [18]. All of these unpinning stresses are between 50 MPa and 150 MPa, which are much lower than all other obstacles. All of the coherent obstacles showed a shearing mechanism during unpinning in the used potential, which means that the unpinning stress needed is determined by the strength of the bonds. The difference between potentials is due to how the potential is describing the Fe-Cr and Cr-Cr interaction. Also the unpinning stress was quite small at the higher temperatures and could vary quite a bit between different runs, which make the numerical values only indicative, but the qualitative results are still valid.

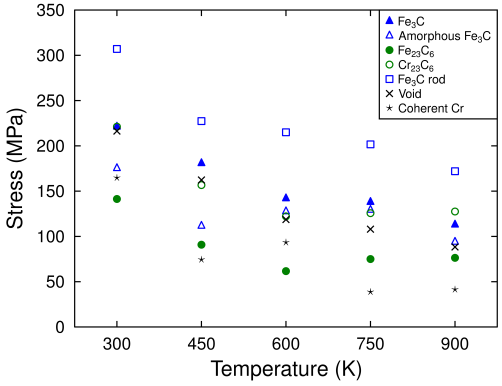

Figure 2. Unpinning stresses for 1 nm obstacles.

The results show that there are clearly three different groupings for the unpinning stresses for the 4 nm obstacles. The hard obstacles (which includes all the carbides), the voids and the coherent obstacles. At the smaller sizes there is not as clear separation of the unpinning stress as for the larger size. The smaller obstacles did still show a similar trend. The smaller obstacles did, in most of the cases, show the same mechanism as for the corresponding large obstacle. The strongest obstacles were those with the Orowan mechanism, and the second strongest the void. The weakest mechanism was the shear, but this mechanism is determined by how the potential is describing the strength of the chosen elements in the obstacle. The other mechanisms are more independent of the obstacles, and the stress required is determined by how the potential describes the matrix. The strength of the shear mechanism is either determined by how strong the non-coherent obstacle is described by the potential, or how the interactions of the coherent obstacle is described. The obstacles of the same kind and with the same unpinning mechanism, did still show some differences in the unpinning stresses. This suggests that to understand the complete unpinning mechanism we still need to account for some other phenomena. These are probably dependent on the nanostructure, and as we showed that some changes in structure or composition can both change the unpinning stress and mechanism.

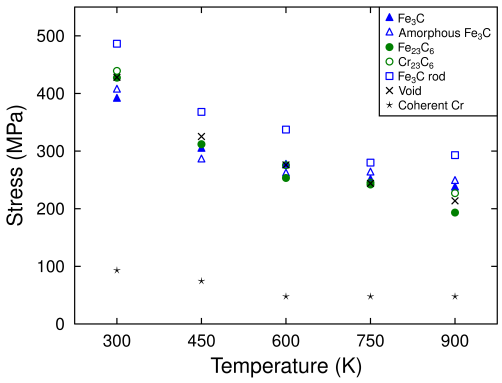

Figure 3. Unpinning stresses for 2 nm obstacles.

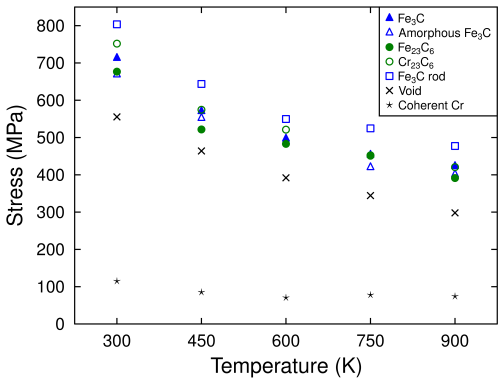

Figure 4. Unpinning stresses for 4 nm obstacles.

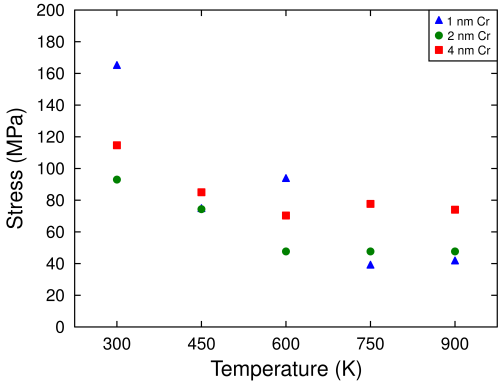

Figure 5. Unpinning stresses for the chromium precipitates.

3.2. Multiple interactions with obstacles

The coherent chromium obstacles were sheared at all temperatures and sizes, which will lead to that after a certain amount of interactions the obstacle will be destroyed. We saw an almost inverse size dependence on the unpinning stress during the first interactions, but during the next interactions we saw that the larger obstacles became much stronger. During the next interactions there is a much larger amount of interface between the Fe- and Cr-atoms, which acted as an obstacle for the dislocation, which led to a much higher unpinning stress for the large obstacles. This indicates that for coherent obstacles the description of the interaction between elements will drastically affect the results.

The evolution of the void during several interactions depended on the amount of absorbed vacancies. For the smallest obstacles the amount of absorbed vacancies was enough for the dislocation to pass without interacting with the obstacles, in form of absorbing vacancies, during the next interactions, leading to an almost pristine void even after several interactions. For the larger voids, the total amount of absorbed vacancies did increase during consecutive interactions, which lead to a larger super jog, eventually large enough to pass without interaction. This also meant that the voids, at least in the beginning, did change their shape at the height where the dislocation interacted with them. The evolution of the unpinning stress did depend mainly on how the dislocation and void was deformed, if a steady state was obtained, a similar unpinning stress was seen during the multiple interactions.

All the different carbides did shear after a few interactions, the 1 nm already at the first interaction and the larger after a few interactions. This means that the precipitates did not withstand the force of the generated Orowan loop(s) plus the dislocation. This shows that even if the obstacles are stronger than the others investigated, they will be destroyed eventually. In most of the cases for the largest obstacle the dislocation absorbed more vacancies/interstitials during consecutive interactions, leading to a smaller effective diameter of the obstacle. For the two smaller obstacles the absorption depended on how exactly the interaction happened, so no clear trend could be seen. For all sizes the carbides were sheared at some height of the obstacle, depending on the super jog magnitude, if the dislocation did not absorb enough vacancies/interstitials to pass without interaction.

The results from multiple interactions with the same obstacles show that it is almost impossible to predict exactly what will happen when non-pristine obstacles will interact with a dislocation with some induced features, like super jogs. In real materials there will be many different combinations of consecutive interaction of perfect and imperfect dislocations with obstacles, that are pristine and non-pristine.

4. Conclusions

In this Article we have investigated the needed stress for edge dislocations to unpin from different kinds of obstacles. The unpinning mechanism, and how it relates to the unpinning

stress, was also determined. We studied and compared obstacles of three different natures (*eg.* hard, void and coherent obstacles), for some of them we studied several different types (*eg.* shape, structure and composition). The effect of size and temperature on the unpinning stress was also determined.

We found, as in previous studies, that for most of the obstacles an increase in temperature will yield a lower unpinning stress and that a larger obstacle will yield a higher unpinning stress. The three different kinds of obstacles each showed a different unpinning mechanism and also different unpinning stresses, accordingly. The stress needed to unpin from obstacles follows the mechanisms in the order of, highest to lowest, Orowan, the absorption and generation associated with voids and shear.

The results show that as a first approximation the obstacles with the same unpinning mechanism will demonstrate similar unpinning stresses. But to understand the full effect and to determine the small differences in the unpinning stress the nanostructure must be considered. We have shown that small changes in the composition or structure can change both the unpinning stress and unpinning mechanism.

Acknowledgments

We would like to thank Krister O. E. Henriksson for the amorphous cementite structures and Dmitry Terentyev for fruitful discussions. This research was funded by the Academy of Finland project SIRDAME (grant no. 259886). We thank the IT Center for Science, CSC, for grants of computational resources. This work has been carried out within the framework of the EUROfusion Consortium and has received funding from the Euratom research and training programme 2014 – 2018 under grant agreement No 633053. The views and opinions expressed herein do not necessarily reflect those of the European Commission.

[1] A. Lehtinen, F. Granberg, L. Laurson, K. Nordlund, M. J. Alava, Multiscale modeling of dislocation-precipitate interactions in fe: From molecular dynamics to discrete dislocations, Phys. Rev. E 93 (2016) 013309.

[2] Y. Xiang, L. T. Cheng, D. J. Srolovitz, W. E, A level set method for dislocation dynamics, Acta Mater. 51 (18) (2003) 5499–5518.

[3] Y. Xiang, D. J. Srolovitz, L. T. Cheng, W. E, Level set simulations of dislocation-particle bypass mechanisms, Acta Mater. 52 (7) (2004) 1745–1760.

[4] Y. Xiang, D. J. Srolovitz, Dislocation climb effects on particle bypass mechanisms, Phil. Mag. 86 (25-26) (2006) 3937–3957.

[5] K. Nordlund, M. Ghaly, R. S. Averback, M. Caturla, T. Diaz de la Rubia, J. Tarus, Defect production in collision cascades in elemental semiconductors and FCC metals, Phys. Rev. B 57 (13) (1998) 7556–7570.

[6] M. Ghaly, K. Nordlund, R. S. Averback, Molecular dynamics investigations of surface damage produced by kiloelectronvolt self-bombardment of solids, Phil. Mag. A 79 (4) (1999) 795.

[7] K. O. E. Henriksson, C. Björkas, K. Nordlund, Atomistic simulations of stainless steels: a many-body potential for the Fe-Cr-C system, J. Phys.: Condens. Matter 25 (44) (2013) 445401.

[8] Y. N. Osetsky, D. J. Bacon, An atomic-level model for studying the dynamics of edge dislocations in metals, Model. Simul. Mater. Sci. Eng. 11 (4) (2003) 427.

[9] H. J. C. Berendsen, J. P. M. Postma, W. F. van Gunsteren, A. DiNola, J. R. Haak, Molecular dynamics with coupling to an external bath, J. Chem. Phys 81 (8) (1984) 3684–3690.

[10] F. Granberg, D. Terentyev, K. Nordlund, Interaction of dislocations with carbides in BCC Fe studied by molecular dynamics, J. Nucl. Mater. 460 (2015) 23–29.

[11] F. Granberg, D. Terentyev, K. Nordlund, Molecular dynamics investigation of the interaction of dislocations with carbides in BCC Fe, Nucl. Instrum. Meth. Phys. Res., Sect. B 352 (2015) 77–80.

[12] A. Stukowski, Visualization and analysis of atomistic simulation data with OVITO-the Open Visualization Tool, Model. Simul. Mater. Sci. Eng. 18 (1) (2010) 015012.

[13] Y. N. Osetsky, D. J. Bacon, Void and precipitate strengthening in a-iron: what can we learn from atomic-level modelling?, J. Nucl. Mater. 323 (23) (2003) 268 – 280.

[14] D. Terentyev, D. J. Bacon, Y. N. Osetsky, Interaction of an edge dislocation with voids in α-iron modelled with different interatomic potentials, J. Phys.: Condens. Matter 20 (44) (2008) 445007.

[15] S. M. Hafez Haghighat, J. Fikar, R. Schäublin, Effect of interatomic potential on the behavior of dislocation-defect interaction simulation in α-Fe, J. Nucl. Mater. 382 (23) (2008) 147–153.

[16] F. Granberg, D. Terentyev, K. O. E. Henriksson, F. Djurabekova, K. Nordlund, Interaction of dislocations with carbides in BCC Fe studied by molecular dynamics, Fusion Sci. Technol. 66 (1) (2014) 283–288.

[17] E. Orowan, in: Symposium of Internal Stresses in Metals and Alloys, Inst. of Metals, London, 1948, p. 451.

[18] G. Bonny, D. Terentyev, L. Malerba, Interaction of screw and edge dislocations with chromium precipitates in ferritic iron: An atomistic study, J. Nucl. Mater. 416 (1-2) (2011) 70–74.